vol. 42, No. 1 (2020) 50-58, DOI: 10.24874/ti.2020.42.01.05

Tribology in Industry

www.tribology.rs

RESEARCH

Effect of Lubrication on the Wear Resistance of Plasma Sprayed Composite Coatings (Al_2O_3+ZrO_2·5CaO)

Abhinav [a,*], R. Ribeiro[a], N. Bodra[a], B. Goala[a], R. Raghav[a], A. Vardhan[a], Md. Mahaboob Ali[a]

[a]*Alliance College of Engineering and Design, Alliance University, Bangalore, Karnataka, India, 562106.*

Keywords:

Ceramic coatings
Lubricant
Abrasive wear

* Corresponding author:

Abhinav
E-mail: abhinavtechno5@gmail.com

Received: 21 June 2019
Revised: 11 August 2019
Accepted: 21 December 2019

A B S T R A C T

Tribological investigations were carried out as per ASTM G134 standard, on plasma sprayed composite coatings (Al_2O_3+ZrO_2·5CaO), under dry and wet abrasive conditions. 20W40 lubricating engine oil was used as a lubricant. Experiments were carried out under normal loads of 10, 15, & 20N, and at a rotational speed of 200 rpm. Scanning Electron Microscopy was used to study the surface characteristics of the as-sprayed and worn out topcoat. Results obtained from the SEM analysis revealed that abrasive wear was mainly governed by third-body abrasion (twinning effect) under dry abrasive conditions. A significant drop in wear rate was realized under the wet lubricated condition, between 10 and 15 N normal loads and a rise in wear rate was observed above 15 N normal load. At higher load, the lubrication was not very effective. At higher loads, It was also observed that the connection between grains improved leading to reduced micro porosity. This caused less abrasion and greater sliding. Experimental data obtained in this work is of good engineering significance as it can be applied to various engineering applications viz. internal combustion engines, cutting tools, etc.

1. INTRODUCTION

In the last three decades, many scientific and technical barriers have been overcome over the traditionally used ceramics viz.Y_2O_3, Al_2O_3, ZrO_2 BeO, SiC, Si_3N_4, WC, AlN etc., either used indigenously or mixed with different stabilizers like MnO, CaO, which are being used in various engineering sectors [1-5]. Despite being brittle in nature, the above ceramics have been successfully used in the oil and gas industry, for aerospace components, cutting tools, ceramic armors, solid oxides fuel cells, internal combustion engines, etc. This is due to their extraordinary passivation against oxidation, high resistance to wear and their significantly high thermal stability against monolithic metals. A ceramic in its pure form does not show any promising results due to its brittle characteristics and limited life span when used in aggressive conditions [1-5]. However, previous research has shown few favorable

results when a pure ceramic was blended scientifically with a metallic powder. This composition is called cermet [5]. In order to extract potential thermo mechanical advantages, researchers are obligated to discover a composition that can be used for high temperature applications (>1000 °C). Ceramics, are considered to be the first choice among scientists and engineers, due to their extraordinary thermo-mechanical properties viz. high microhardness, high resistance to wear and tear, chemical inertness, extraordinarily strong ionic and covalent bonding, high structural integrity among the constituent elements in the composite especially in an aggressive environment (high temperature, corrosion and friction). On the other hand, a limited thermo mechanical property bounds the applications of monolithic metals, compared to ceramics. It has been also observed that atomic bonding in ceramics is mostly governed by ionic-covalent bonds (the presence of both kinds, leads to easy blending of ceramic powder with metallic powder). In the case of metals, only the metallic bond determines the strength of the material. This is the reason for the applications of ceramics, increasing greatly over conventional metals [6].

After an extensive literature survey, it was observed that the wear of the coated samples primarily depended on the coating microstructure, porosity, hardness, coating thickness, and operational parameters such as load, velocity, and friction [7]. Earlier investigations demonstrated that compositions like ZrO_2+8%Y_2O_3, ZrO_2+20% Y_2O_3, and Al_2O_3+ZrO_2 coatings have superior and extended wear life against cast-iron [8,9]. It was commonly found that the wear resistance of a material is strictly allied to its coating defects, microhardness, toughness, and the ratio of its hardness to the hardness of abrasive materials [9]. In addition to hardness and toughness, the microstructure of ceramics, especially grain size, has an immense influence on its wear resistance [10-12]. It has also been found that the composite phase has a significant effect on the process of wear [13]. It has been generally recognized that the wear of polycrystalline alumina varies significantly with mean grain size. The wear rate increases rapidly with the increase in its grain size [14-15]. Earlier investigations showed that fine-grained ceramics have lower wear rates in comparison with that of coarse-grained ceramics [15]. Y. Wang [16] had investigated the abrasive wear characteristics of plasma sprayed nanostructured alumina-titania coatings (250 to 600 μm thick) on a mild steel substrate. His studies showed that the worn surfaces of conventional coatings exhibited grooves, plastic deformation, and micro fractures. It has, however been found that the governing mechanism of material subtraction of nanostructured coatings is due to grain dislodgement [17]. Lei Fan carried out wear studies on zirconia toughened alumina (ZTA) reinforced iron matrix composites and found that a composite with 30 vol. % of ZTA particles exhibited the best wear resistance during the sliding wear test [18]. Friction and wear analysis were also carried out on Fe-Ni alloy matrix ($Fe_{70}Ni_{30}$) reinforced with varying wt.% of ZrO_2 particles, and it was found that the addition of 10 wt.% of ZrO_2 improved the wear resistance and reduced the plastic flow in the wear process [19].

In recent times, a number of experimental investigations have been carried out on alumina plus calcia stabilized zirconia (Al_2O_3+ZrO_2·5CaO) ceramic composite, mostly as a topcoat [20, 21]. It has shown remarkable results viz. passivation against corrosion at higher coating thicknesses between 200 to 300 μm. There was significant improvement in the adhesion strength observed (49.33 MPa). Micro porosity reduced by ~3 % as compared to a reduction of ~10 % for Al_2O_3. There was also an improved life span (312 cycles of heating and cooling in the interval of half an hour) of the topcoat when the coating thickness was increased to 300 μm, and was subjected to thermal cyclic tests [20,21]. It is understood that the extended application and understanding of this ceramic composite is still under investigation and needs add-on investigations and development.

Due to the mixed response of ceramic and cermet, the researchers searched for alternate composite compositions. Also, extended research is still under way on the blended composite Al_2O_3+ZrO_2·5CaO. In this context, an investigation was carried out to examine the tribological behavior of this composite coating under dry and wet conditions and under different loading conditions. Their wear rates were compared. The best performance, (resistance to wear) at the given loads were also determined and can be applied to Internal combustion engine applications (not limited to).

Table 1. Material composition and operating parameters.

Materials	Primary gas (Argon) Pressure (Bar)	Secondary gas (Hydrogen) Pressure (Bar)	Carrier gas Argon Flow (lpm)	Current (amps)	Voltage (Volts)	Spray distance (mm)
Al_2O_3+ZrO_2·5CaO	3.7	3.45	35	500	65	65-76
Fe38Ni10Al	6.9	3.30	35	500	65	50-76
Al25Fe7Cr5Ni	6.9	3.30	35	500	65	50-76

2. METHODOLOGY

2.1 Specimen preparation

The atmospheric plasma sprayed coating technique was adopted to coat the specimen. Eighteen specimens (coatings developed on cast iron substrate) were prepared for tribological study. Approximate dimensions of each plate were tailored for the experimental trials. The coated specimen is shown in Fig. 1.

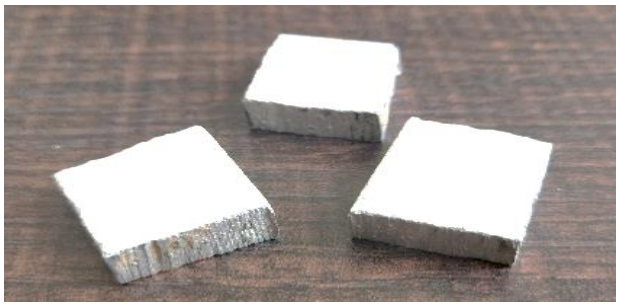

Fig. 1. Plasma sprayed coated specimen (15×15 mm^2).

The material composition of the topcoat, bond coats applied on the Cast iron substrate and operating parameters are shown in Table 1.

2.2 Coating characterization

Detailed microstructure examinations, particle size determination of as-sprayed and worn out surfaces were carried out using a Hitachi scanning electron microscope. The specifications of the model are given in Table 2.

Table 2. Scanning electron microscope specification.

SEM Specification	
Make	Hitachi
Model	SU 3500N
Detector	SE and BSE
Resolution	7nm SE image at 3 kv, 10 nm BSE image at 5 kv
Voltage	Variable (up to 30kv)
Magnification	300000 X

The average value of top coating thickness was determined to be 200±32 μm (Fig. 2).

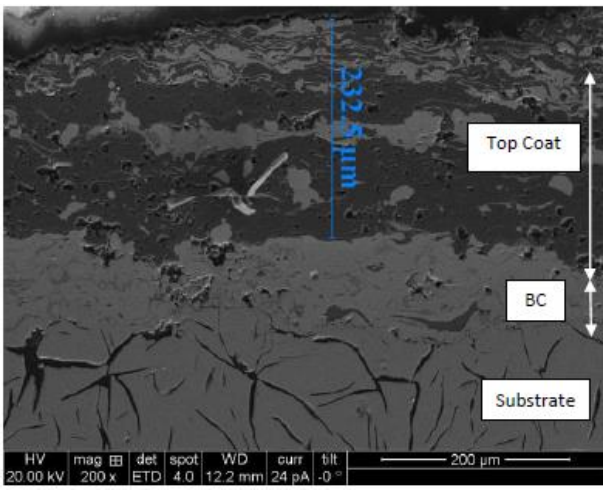

Fig. 2. Schematic of topcoat thickness.

The schematic of the coating thickness is shown and discussed in section 3.1.

2.3 Wear analysis

ASTM G132 standard [22] was adopted to conduct Pin-On-Disk abrasive wear tests. An abrasive disk f grain size 60 μm was mounted on the circular disk to simulate the abrasive condition. During the tribo test, height loss (reduction in the top coating thickness), was obtained directly from the data acquisition system connected to a computer, refer Fig. 3a.

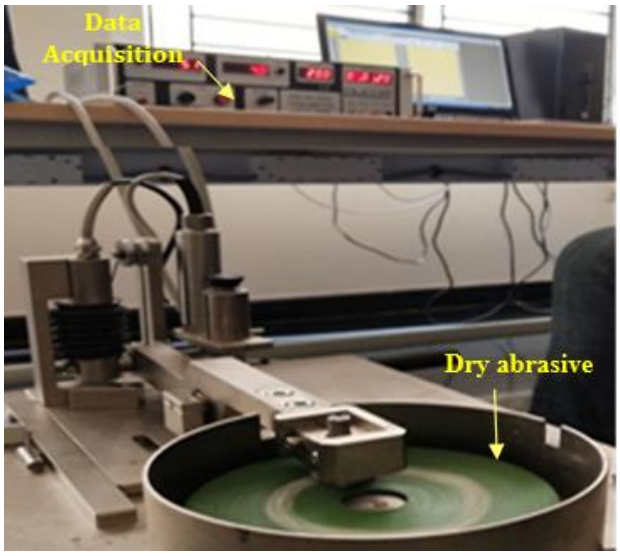

(a)

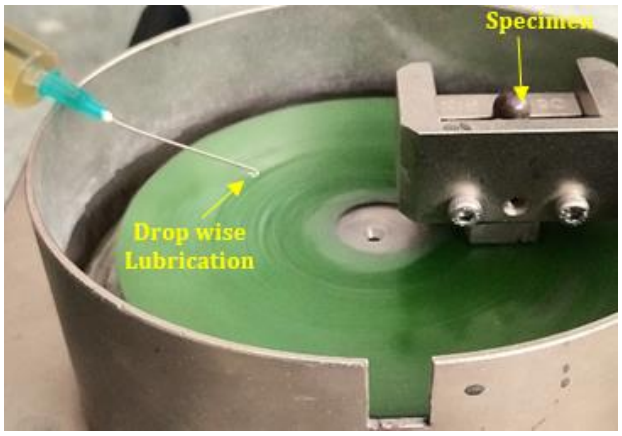

(b)

Fig. 3. (a) Schematic of tribological setup in Dry condition and (b) Schematic of tribological setup in Wet condition.

The data obtained from the software was incorporated in the formula to determine the cumulative volume loss over the specified area. The test was carried out at three different normal loads, viz. 10, 15 and 20 N. Three trials were done at each load under dry and wet abrasive conditions and the average wear rate was determined. An ordinary syringe was used to maintain a constant drop-wise flow of lubricant (Engine Oil) on the rotating disk, shown in Fig. 3b. The operating parameters considered during the experiment are shown in Table 3.

Table 3. Tribological operating parameter.

Tribological Test Parameters	
Normal load	10,15 and 20 N
Disk rotational speed	200 rpm
Track diameter	60 mm
Abrasive disk grain size	60 µm
Type of lubricant (commercial)	20W40 Engine Oil

The formulae used to calculate specific wear rate are as follows:

1. Cross-sectional area = (Sides^2) in (mm^2).
2. Volume loss = (Cross-sectional area × Average height loss) in (mm^3). Average height loss measurement was taken from the data generated by the software.
3. Sliding Distance = [Sliding Velocity (m/s)× Time(s)] in (m).
4. Sliding Velocity = [(2×Pi×N×r)/ (60×1000)], in (m/s). Where: N= Rotational Speed of a Disk in (rpm); r = Track radius in (mm).
5. Wear rate = (Volume loss/ Sliding Distance) in (mm^3/m).
6. Specific wear rate (SWR.) = (Wear rate / Normal Load) in (mm^3/mN).

3. RESULTS AND DISCUSSION

3.1 Coating Characterization

As-sprayed SEM images clearly showed interlocked flattened grains, suspended particles, localized agglomerated grains, and connected microvoids (Fig. 4a under 15 N normal load. Post wear analysis showed a flattened surface with partially open voids and micropores (Fig. 4b).

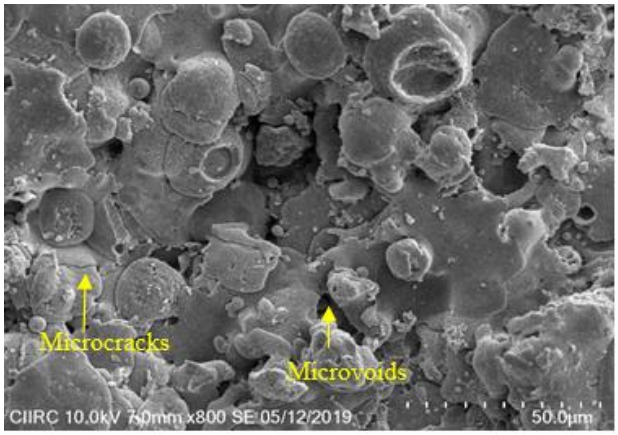

(a)

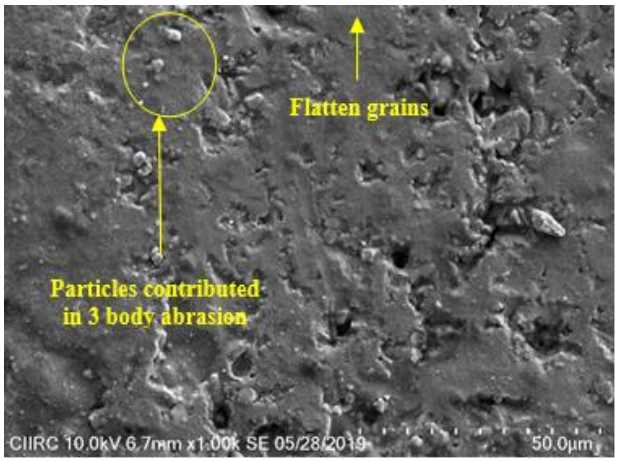

(b)

Fig. 4. (a) SEM micrographs of topcoat status of As-sprayed coatings, and (b) SEM micrographs of topcoat Post wear, dry condition at 15 N normal load.

The average microhardness for the topcoat was measured and was found to be 668.98 HV and the micrograph of the same is shown in Fig. 5. Under the wet condition, the topcoat

was found to glide over the tribofilm manifested between the mating surfaces for normal loads of 10 N and 15N. Less severe stress marks were seen on the wear track for these loads (10-15 N).

Fig. 5. SEM micrograph showing micro indentation at the topcoat with microhardness value 668.98 $HV_{0.1}$.

Figure 6a shows the SEM image of the as-sprayed coating. Post dry and wet SEM micrographs are shown in Figs. 6b and 6c respectively, for a normal load of 10 N. In the as-sprayed coatings, the particle size ranged from 1.81 µm to 8.20 µm (Fig. 6a), on the other hand, the particle size significantly reduced during dry abrasive wear (~1.69 -~2.36 µm), refer to Fig. 6b. A similar range of the particle size was observed (~1.43-2.70 µm), under wet abrasive conditions; refer to Fig. 6c.

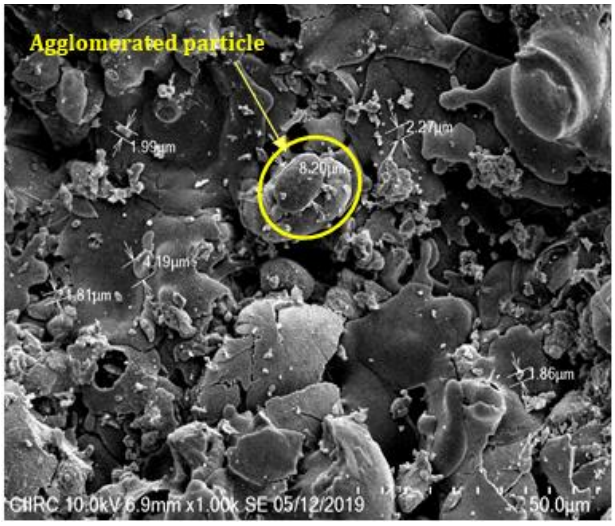

(a)

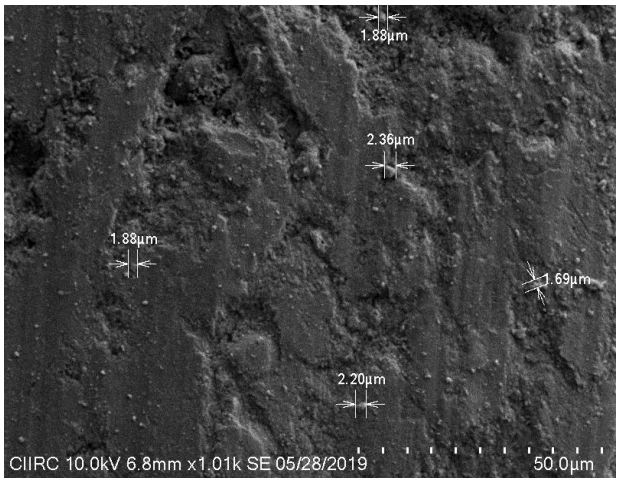

(b)

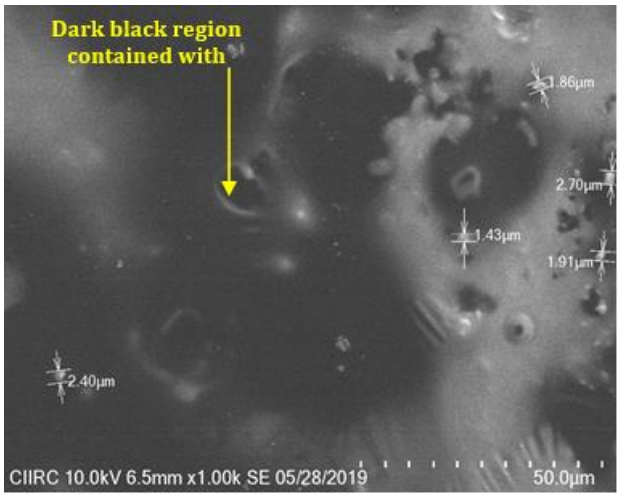

(c)

Fig. 6. (a) As-sprayed topcoat particle size distribution, (b) Dry-Post wear topcoat particle size for 10 N normal load, and (c) Wet- post wear topcoat particle size at 10 N normal load.

In earlier research, reduction in the particle size was found to have direct consequences on the wear rate and it has been also recognized that the wear of polycrystalline alumina varied significantly with mean particle size. The wear rate increased rapidly with the rise in its grain size [23]. Earlier investigations have indicated that fine-grained ceramics have lower wear rates in comparison with that of coarse-grained ceramics, in both sliding and erosive wear [24-25]. For example, reducing the grain size of Al_2O_3 from 20 to 4 µm has led to a five-fold increase in transition time from a moderate wear stage characterized by plastic deformation and grooving to a rapid wear stage characterized by micro fracture and grain pull-out [26]. The present work also supports the above statements. The smaller the grain size, the finer would be the flaws and hence a higher

magnitude of external stress is required to induce grain boundary cracking and grain pull-out. Smaller grains are more resistant to fracture [27-28]. The topcoat integrity was manifested with a reduced scar at 10 N and 15 N normal load, and measured in the range of 66.9-81 μm under wet abrasive conditions, compared to an increase in wear track width observed between 172 to 181 μm under the dry abrasive wear conditions, refer to Figs. 7a and 7b.

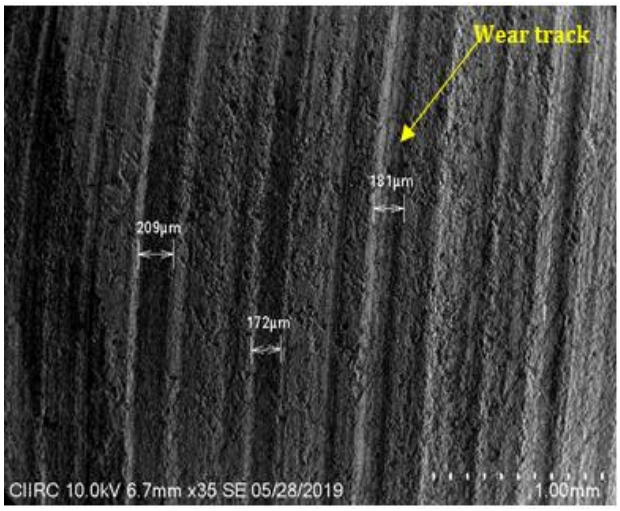

(a)

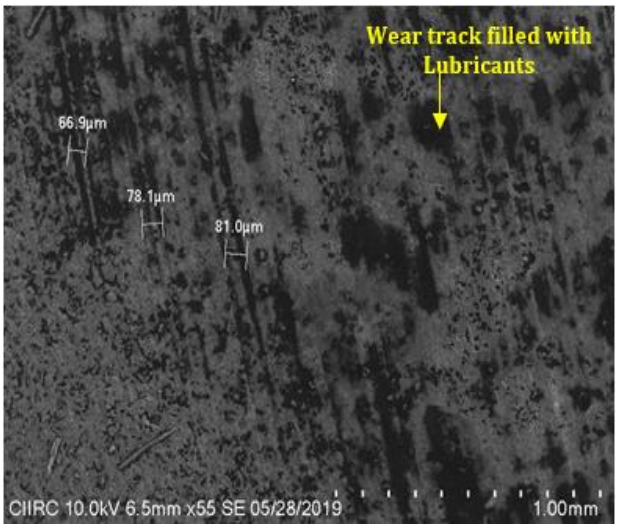

(b)

Fig. 7. (a) SEM micrograph show wear track in dry condition at 15 N normal load, and (b) SEM micrograph show wear track in wet condition at 15 N normal load.

From the SEM micrographs Figs. 6c and 7b, it has been observed that micro voids and micro porosity can assist in developing a tribofilm between the asperities and can significantly reduce wear between the mating parts and may enhance the life of the topcoat.

3.2 Wear analysis

Minor scars and negligible wear track widths were observed at lower normal loads of 10N and 15 N, under wet condition (Figs. 6c and 7b). Referring to Table 3, at these loads, the average wear rate was measured and found to be 0.047 and 0.051×10^{-6} mm^3/m respectively. However, in the case of dry wear, at 10N normal load, the wear rate was observed as 0.026×10^{-6} mm^3/m and 0.107×10^{-6} mm^3/m at 15N normal load. The average wear rate at higher load (20 N) was found to be 0.264×10^{-6} mm^3/m under dry conditions and 0.233×10^{-6} mm^3/m under wet conditions. These values are a significant increase compared to their counterparts at 10N and 15 N. In Fig. 8a, it is seen that there is dislodgement of particles at 10 N load, under dry condition. These particles cause third body abrasion, which is evident under normal loads of 15 N and 20 N, under dry condition (Figs. 8b and 8c). At lower loads of 10 N and 15 N, it has been observed that a hydrodynamic lubricant layer remained in contact with the asperities but was not present at a higher load of 20 N.

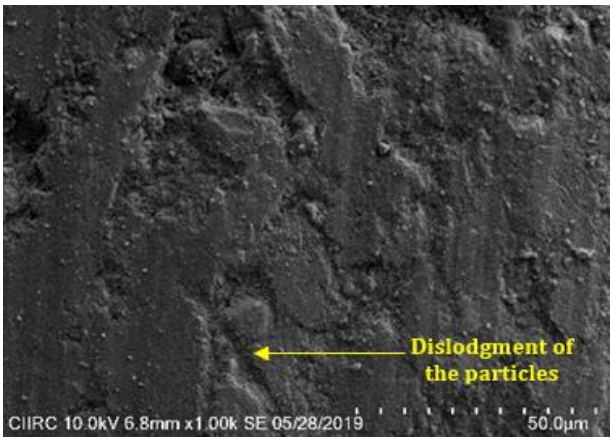

(a)

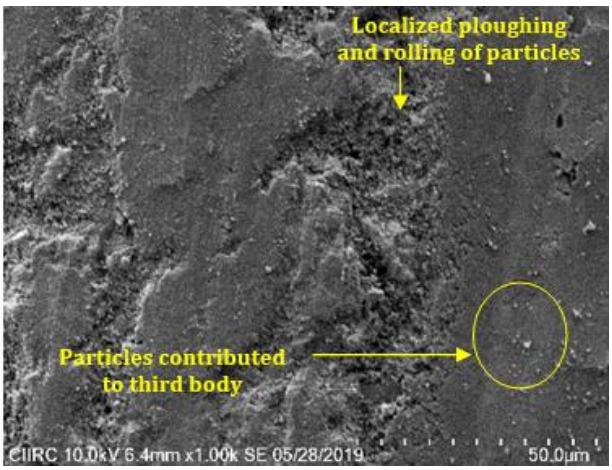

(b)

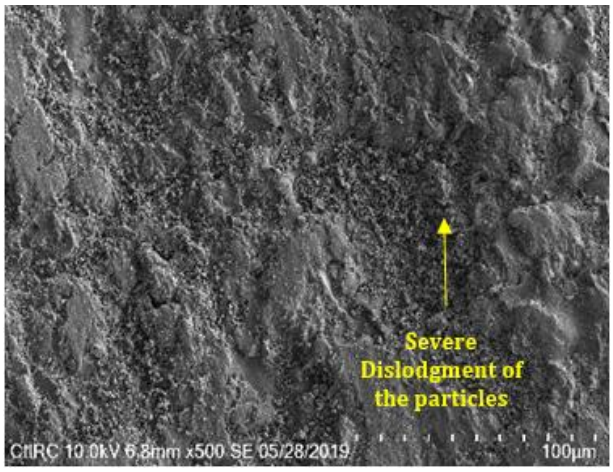

(c)

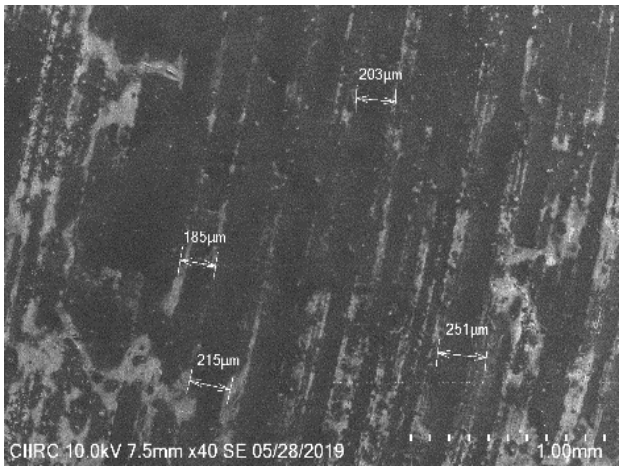

(b)

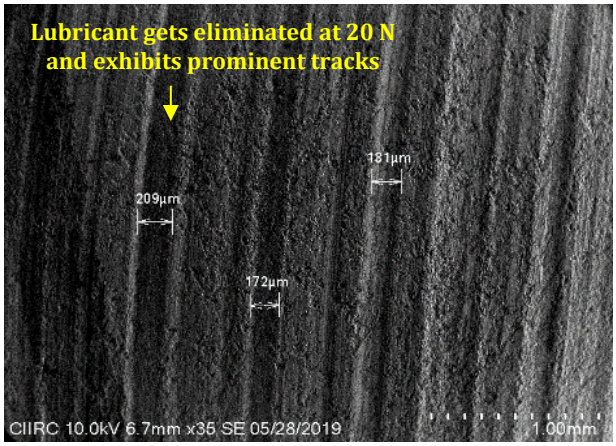

(c)

Fig. 8. (a) SEM micrograph show dry- post wear, worn out status of the topcoat at 10 N normal load, (b) SEM micrograph show dry- post wear, worn out status of the topcoat at 15 N normal load, and (c) SEM micrograph show dry- post wear, worn out status of the topcoat at 20 N normal load.

The same can be observed in the SEM micrographs, refer Figs. 9a, 9b and 9c. The measured values of wear rate were found to support the SEM micrographs. At 10 N and 15 N normal loads, the plastically deformed zones (highly stressed) were found to be occupied with the lubricant, thus forming a tribofilm between the interacting asperities and showed less wear or wear rate at 10 N and 15 N normal loads (refer to Figs. 9a and 9b).

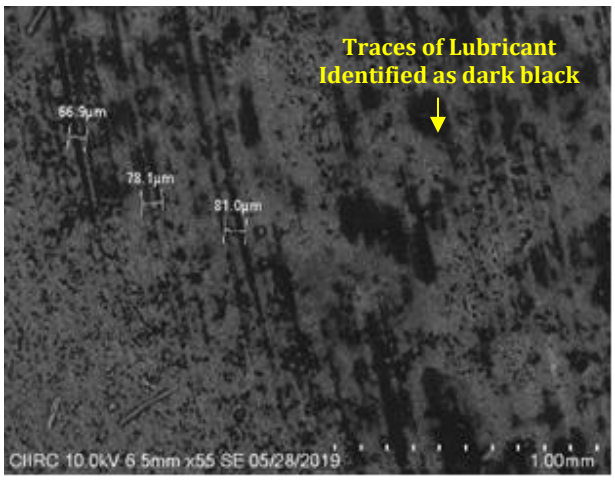

(a)

Fig. 9. (a) SEM micrograph show wet- post wear status of the topcoat at 10 N normal load, (b) SEM micrograph show wet- post wear status of the topcoat at 15 N normal load, and (c) SEM micrograph show wet- post wear status of the topcoat at 20 N normal load.

It has been noticed that at 20 N, the tribofilm got eliminated and the sample was left with a severe band of plastically deformed tracks (Fig. 9c). The reason for this can be attributed to high contact stress established between the abrasive particles on the disk with the coating asperities. Comparative results are shown in Table 3, for the different normal loads. Under the wet lubrication condition, at 20 N, the structural integrity was found to slacken due to a dislocation and twinning effect, Fig. 9c. The twining effect leads to ploughing and rolling of particles between the mating surfaces (three body abrasion).

Table 3. Average wear rate calculation with and without lubricant at the normal load of 10, 15 and 20 N.

Load in (N)	Avg. wear rate without lubricant $mm^3/m \times 10^{-6}$	Avg. wear rate with lubricant $mm^3/m \times 10^{-6}$
10	0.026	0.047
15	0.107	0.051
20	0.264	0.233

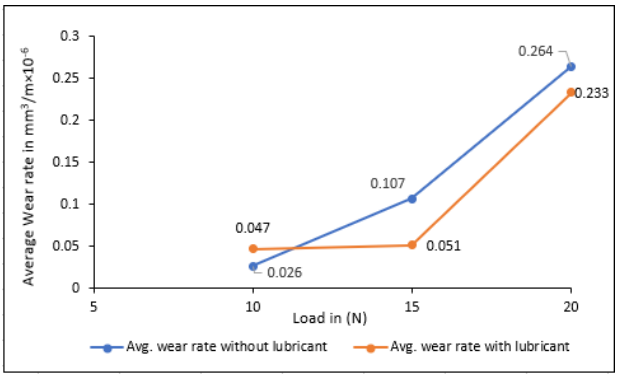

Fig. 10. Comparative analysis of average wear rate with and without lubricant at normal loads of 10, 15 and 20 N.

The average wear rates with and without lubricant were also compared and shown graphically in Fig. 10. An almost equal wear rate was observed at 10 N and 15 N normal loads. In the case of the dry abrasive condition, increased wear rate was observed with a gradually increasing slope. In both dry and wet conditions, slope increased above 15 N normal loads. The reason for increasing slope can be attributed to the continuous formation of fragmented particles which remain between the mating surface asperities during the test period. This can be observed in the SEM micrographs for 20 N normal load (refer to Figs. 8a, 8b and 8c). During the friction and wear study, it was found that at 10N normal load, the best performance can be expected with and without lubricant.

4. CONCLUSION

The important findings related to the tribological study of dry and wet abrasive wear of the present topcoat Al_2O_3+ZrO_2·5CaO are as follows:

1. The Present coating has the potential to exhibit good antiwear characteristics between 10 to 15N normal loads, as observed from wear calculations and the SEM micrographs, under the wet abrasive conditions.
2. At 15N normal load, significantly less wear rate (0.051×10^{-6} mm³/m) was observed in the case of the wet abrasive condition. The use of lubricant therefore has a significant role in altering the wear rate at 15N normal load. Under dry condition, the wear rate was found to be significantly higher at 0.107 $\times10^{-6}$ mm³/m.
3. The effect of lubrication gets eliminated at the higher load of 20N under the wet abrasive condition. The wear rate calculations were found to support the SEM micrographs (Severe wear tracks, stress marks).

Acknowledgement

We would like to express sincere thanks to CMTI, CIIRC, and Alliance University, Bangalore for offering research facilities for this research work.

REFERENCES

[1] S. Jahanmir, *Tribological Applications for Advanced Ceramics*, Symposium S–New Materials Approaches to Tribology: Theory and Applications, vol. 140, pp. 285-291, 2011, doi: 10.1557/PROC-140-285

[2] U. Taffner, V. Carle, U. Schafer, *Preparation and Microstructural Analysis of High-Performance Ceramics*, Metallography and Microstructures, ASM International, vol. 9, pp. 1057-1066, 2004.

[3] J.A. Fernie, R.A.L. Drew, K.M. Knowels, *Joining of Engineering Ceramics*, International Materials Reviews, vol. 5, iss. 5, pp. 283-331, 2009, doi: 10.1179/174328009X461078

[4] D. Munz, T. Fett, *Ceramics: Mechanical Properties, Failure Behaviour, Materials Selection*. Springer, 2001.

[5] Abhinav, N. Krishnamurthy, R. Jain, *Corrosion Kinetics of Al_2O_3+ZrO_2·5CaO Coatings applied on Gray Cast Iron Substrate*, Ceramics International, vol. 43, iss. 17, pp. 15708-15713, 2017, doi: 10.1016/j.ceramint.2017.08.131

[6] M.R. Loghman-Estarki, M. Hajizadeh-Oghaz, H. Edris, R. Shoja Razavi, A. Ghasemi, Z. Valefi, H. Jamali, *Plasma-sprayed nanostructured Scandia-yttria and ceria-yttria codoped zirconia coatings: Microstructure, bonding strength and thermal insulation properties*, Ceramics International, vol. 44, no. 11, pp. 12042-12047, 2018, doi: 10.1016/j.ceramint.2018.03.204

[7] P.J. Blau, *Friction and wear transitions of materials*. Noyes publications, Park Ridge, N.J., USA, 1989.

[8] N. Krishnamurthy, M.S. Murali, P.G. Mukunda, M.R. Ramesh, *Characterization and wear behavior of plasma-sprayed Al_2O_3 and ZrO25CaO coatings on cast iron substrate*, Journal of Materials Science, vol. 45, iss. 3, pp. 850–858, 2010, doi: 10.1007/s10853-009-4009-3

[9] N. Krishnamurthy, M. S. Prashantha Reddy, H.P. Raju, H.S. Manohar, *A Study of Parameters*

Affecting Wear Resistance of Alumina and Yttria Stabilized Zirconia Composite Coatings on Al-6061 Substrate, International Scholarly Research Network ISRN Ceramics, vol. 2012, no. 585892, p. 13, 2012, doi: 10.5402/2012/585892

[10] G.J. Gore J.D. Gates, *Effect of hardness on three very different forms of wear*, Wear, vol. 203–204, pp. 544-563, 1997, doi: 10.1016/S00431648(96)07414-5

[11] I. Sevim, I.B. Eryureket, *Effect of fracture toughness on abrasive wear resistance of steels,* Materials & Design, vol. 27, iss. 10, pp. 911-919, 2006, doi: 10.1016/j.matdes.2005.03.009

[12] L. Zhou, G. Liu, Z. Han, K. Lu, *Grain size effect on wear resistance of a nanostructured AISI 52100 steel*, Scripta Materialia, vol. 58, iss. 6, pp. 445-448, 2008, doi: 10.1016/j.scriptamat.2007.10.034

[13] A.V. Makarov, N.N. Soboleva, I. Yu. Maligina*, Role of the strengthening phases in abrasive wear resistance of laser-clad NiCrBSi coatings*, Journal of Friction and Wear, vol. 38, iss. 4, pp. 272–278, 2017, doi: 10.3103/S1068366617040080

[14] H. Liu, M.E. Fine, *Modelling of grain size dependent microstructure controlled sliding wear in polycrystalline alumina*, Journal of the American Ceramic Society, vol. 76, iss. 9, pp. 2393-2396, 1993, doi: 10.1111/j.1151-2916.1993.tb07786.x

[15] S-J. Cho, B.J. Hockey, B.R. Lawn, S.J. Bennison*, Grain size and R-curve effects in the abrasive wear of alumina*, Journal of the American Ceramic Society, vol. 72, iss. 7, pp. 1249-1252, 1989, doi: 10.1111/j.1151-2916.1989.tb09718.x

[16] Y. Wang, S. Jiang, M. Wang, S. Wang, T.D. Xiao, P.R. Strutt, *Abrasive wear characteristics of plasma sprayed nanostructured alumina/titania coatings,* Wear, vol. 237, iss. 2, pp. 176-185, 2000, doi: 10.1016/S0043-1648(99)00323-3

[17] H.H.K. Xu, S. Jahanmir, *Microfracture and material removal in scratching of alumina*, Journal of Materials Science, vol. 30, pp. 2235-2247, 1995, doi: 10.1007/BF01184566

[18] L. Fan, *Wear Behavior of ZTA Reinforced Iron Matrix Composites, in Proceedings of the 7th International Conference on Fracture Fatigue and Wear*, FFW 2018, 9-10 July 2018, Springer, Singapore, pp. 732-746.

[19] N. Singh, O. Parkash, D. Kumar, *Wear Behavior of ZrO_2 Particle Reinforced (Fe,Ni) Matrix Composite*, in Proceedings of the 7th International Conference on Fracture Fatigue and Wear, FFW-2018, 9-10 July, 2018, Springer, Singapore, pp. 682-690.

[20] Abhinav, N. Krishnamurthy, R. Jain, P.H.V.S. Talpasai, *An elucidation on adhesive strength of Al_2O_3 and $ZrO_2{\cdot}5CaO$ composite coating applied on Al-6061 & CI substrates*, International Journal of Mechanical and Production Engineering Research and Development, special iss., pp. 91-98, 2018, doi: 10.13140/RG.2.2.17125.45281

[21] Abhinav, N.K. Murthy, A.J. Nair, *Thermochemical and Thermomechanical Study on Composite Coatings (Al 2O 3+ZrO 2•5CaO),* Proceedings of Second International Conference on Emerging Trends In Science & Technologies For Engineering Systems (ICETSE-2019), SJC Institute of Technology, Chickballapur, Karnataka, India, 17th and 18th May 2019, pp. 948-954, 2019, doi: 10.2139/ssrn.3511933

[22] ASTM G132, Standard Test Method for Pin Abrasion Testing, 1995.

[23] H. Liu, M.E. Fine*, Modelling of grain size dependent microstructure controlled sliding wear in polycrystalline alumina*, Journal of the American Ceramic Society, vol. 76, iss. 9, pp. 2392-2396, 1993, doi: 10.1111/j.1151-2916.1993.tb07786.x

[24] S.M. Weiderhorn, B.J. Hockey, *Effect of material parameters on the erosion resistance of brittle materials*, Journal of Materials Science, vol. 18, pp. 766-780, 1983, doi: 10.1007/BF00745575

[25] S. Lathabai, D.C. Pender, *Microstructural influence in slurry erosion of ceramics*, Wear, vol. 189, iss. 1-2, pp. 122-135, 1995, doi: 10.1016/0043-1648(95)06679-9

[26] S-J. Cho, B.J. Hockey, B.R. Lawn, S.J. Bennison, *Grain size and R-curve effects in the abrasive wear of alumina*, Journal of the American Ceramic Society, vol. 72, iss. 7, pp. 1249-1252, 1989, doi: 10.1111/j.1151-2916.1989.tb09718.x

[27] K.-H.Z. Ghar, *Modelling and microstructural modifications of alumina ceramic for improved tribological properties*, Wear, vol. 200, no. 1-2, pp. 215-224, 1996, doi: 10.1016/S0043-1648(96)07293-6

[28] K. Jia, T.E. Fischer, *Abrasion resistance of nanostructured and conventional cemented carbides*, Wear, vol. 200, no. 1-2, pp. 206-214, 1996, doi: 10.1016/S0043-1648(96)07277-8